On the Properties of Loop-Flower Basis Functions

Yibei Hou [1], Gaobiao Xiao [1], and Jinpeng Fang [2]

[1] Key Laboratory of Ministry of Education
Design and Electromagnetic Compatibility of High-Speed Electronic Systems
Shanghai Jiao Tong University, Shanghai, 200240, China
yibhou@sjtu.edu.cn, gaobiaoxiao@sjtu.edu.cn

[2] Shanghai Key Laboratory
Electromagnetic Environmental Effects for Aerospace Vehicle
Shanghai, China
jpfang1129@sina.com

Abstract ─ This paper presents a mathematical analysis of loop-flower basis functions which are adopted to cure low frequency breakdown in integral equations for solving electromagnetic scattering problems. Flower basis functions will be analyzed based on RWG-connected graph generated according to RWG basis functions. This paper will also explore the conditioning behavior of loop-flower Gram matrices which greatly contributes to the whole conditioning of electric field integral equation. The performance of loop-flower basis functions is confirmed by numerical results that show fast convergence rate of iteration solvers, which are better than those of loop-star basis functions.

Index Terms ─ Conditioning behavior, electromagnetic scattering, Gram matrices, loop-flower basis functions, low frequency breakdown.

I. INTRODUCTION

Electric field integral equations (EFIEs) are usually discretized by using Method of Moment (MoM), which is widely adopted to analyze electromagnetic problems in computational electromagnetics community. To numerically solve EFIE, the surface of the object is often discretized as simple elements such as triangles and quadrilaterals. Rao-Wilton-Glisson (RWG) basis functions are popular to expand surface electric and magnetic currents among all divergence-conforming vector basis functions. However, the use of RWG basis functions for the EFIE exhibits low frequency breakdown, that is to say, at very low frequencies the discretized EFIE matrix system is highly ill-conditioned, and hence is difficult to be solved accurately and efficiently [1,2]. In addition, when the EFIE is discretized with boundary elements of average geometry diameter h, the resulting matrix has a condition number growing as $(kh)^{-2}$, where k is the wavenumber. Moreover, the impedance matrices resulting from EFIE tend to be ill-conditioned when derived from dense meshes whose average lengths are much smaller than the wavelength of the excitation [1,3].

Performing quasi-Helmholtz decomposition can cure the low frequency breakdown effectively. Various quasi-Helmholtz decompositions such as loop-star (LS) basis functions, loop-tree (LT) basis functions and so on, have been proposed in the past few years [4-8]. These quasi-Helmholtz decompositions forcibly separate the surface currents into the solenoidal part and the irrotational one properly at low frequencies. Moreover, a frequency scaling scheme is also implemented to obtain stable systems. Hence, both two parts of the currents can be handled correctly. Even though the quasi-Helmholtz decomposition is an efficient method to overcome low frequency breakdown, it cannot improve the conditioning of the EFIE operator when meshes are dense. Recently, an efficient Calderón multiplicative preconditioner [9] has been proposed to solve the above problems and introduce the Buffa-Christiansen (BC) basis functions [10] to avoid the singular Gram matrix. BC basis functions can be expressed by the linear combinations of the RWG basis functions defined on the barycentric refined triangular mesh, and thus additional memory is required. Furthermore, the Calderón preconditioner with BC basis functions may fail at very low frequencies without other special treatments [11].

Loop-flower (LF) basis functions are proposed to implement Calderón preconditioner directly in [11]. The left and right EFIE operators are both discretized by using loop-flower basis functions. Consequently, there is no need to refine the original mesh to generate BC basis functions. Besides, loop and flower basis functions are both defined on nodes, which compress the degrees of freedom (DoF) compared with RWG basis functions. When the loop-flower basis functions are implemented

Submitted On: October 19, 2014
Accepted On: April 20, 2015

in EFIE, the convergence rate of iterations can be estimated by analyzing the conditioning of EFIE system, in which the conditioning of loop-flower Gram matrix is the sole cause of the overall condition number of the decomposed equation. Preliminary results of the conditioning properties of loop-flower Gram matrices are presented in [12].

In this paper, we present an analysis of flower basis functions from a perspective of graph theory. Hereafter, we will use the terminology 'RWG-connected' to denote the relationship between two nodes which are free vertexes of a RWG basis function, as is defined in [11]. The graph generated according to RWG-connected relations has a similar behavior compared with the edge-connected graph. In addition, Gram matrices associated with the loop-flower basis functions are analyzed using graph Laplacian matrices as auxiliary tools. The performance of loop-flower basis functions in comparison with loop-star basis functions is also presented in this work.

II. LOOP-FLOWER BASIS FUNCTIONS

Loop-flower basis functions arise from the need to perform quasi-Helmholtz decomposition. In this method, loop basis functions are used to expand the solenoidal currents, while flower basis functions are for the irrotational parts [11-13]. A loop basis function is defined on each interior vertex v_j, which is shown in the left one of Fig. 1. Loop basis functions can be written as:

$$\boldsymbol{f}_j^L(\boldsymbol{r}) = \sum_{i=1}^{N} \Lambda_{i,j} \boldsymbol{f}_i'(\boldsymbol{r}), \tag{1}$$

where N represents the number of RWG basis functions, $\bar{\bar{\boldsymbol{\Lambda}}}=\left[\Lambda_{ij}\right]$ is the loop to RWG transformation matrix and $\boldsymbol{f}'(\boldsymbol{r})$ means the standard RWG basis function divided by the common edge length.

A loop basis function maintains a direct relationship with the piecewise linear Lagrange basis function [12] (or the nodal basis function) associated with vertex in the FEM community. Consequently, loop basis function can be also rewritten by:

$$\boldsymbol{f}_p^L(\boldsymbol{r}) = \nabla \times \hat{\boldsymbol{n}}_r \lambda_p(\mathbf{r}) = \hat{\boldsymbol{n}}_r \times \nabla \lambda_p(\boldsymbol{r}), \tag{2}$$

in which, $\hat{\boldsymbol{n}}_r$ denotes the outward normal unit vector and $\lambda_p(\boldsymbol{r})$ is piecewise linear Lagrange basis function. It is easy to verify that the gradient of $\lambda_p(\boldsymbol{r})$ is divergence-conforming, while $\hat{\boldsymbol{n}}_r \times \nabla \lambda_p(\boldsymbol{r})$ is curl- conforming.

A flower basis function is also defined on the node v_j, like a loop basis function, as depicted in the right one of Fig. 1. Its support covers all the RWG bases that share the reference node v_j as one free vertex. It can be explicitly expressed by:

$$\boldsymbol{f}_j^F(\boldsymbol{r}) = \sum_{i=1}^{N} F_{i,j} \boldsymbol{f}_i(\boldsymbol{r}), \tag{3}$$

where $\bar{\bar{\mathbf{F}}}=\left[F_{ij}\right]$ stands for the flower to RWG transformation matrix. The reference direction of flower basis function points away from the reference node.

Since the space spanned by flower basis functions is a subspace of the space spanned by star basis functions, the accuracy of the EFIE solver using loop-flower bases can be affected by the mesh quality. To improve the accuracy, the flower basis function is slightly modified and constructed by using RWG bases without normalization directly.

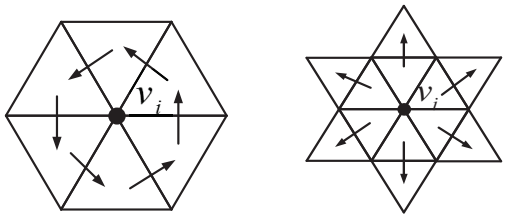

Fig. 1. Loop and flower basis function.

In order to proceed, we need to summarize a number of preliminary facts. Recall that the Laplacian matrix of the graph G is the $N \times N$ symmetric matrix $\bar{\bar{\mathbf{L}}}$:

$$\bar{\bar{\mathbf{L}}} = \bar{\bar{\mathbf{D}}} - \bar{\bar{\mathbf{A}}}, \tag{4}$$

in which, $\bar{\bar{\mathbf{A}}}$ is the adjacency matrix of the graph G and $\bar{\bar{\mathbf{D}}}$ stands for the diagonal matrix diag(d_1, d_2, …, d_m) whose diagonal entries are the degree of the corresponding vertices [14-16]. Since all the sums of rows in $\bar{\bar{\mathbf{L}}}$ equal to zero, the matrix $\bar{\bar{\mathbf{L}}}$ has a zero eigenvalue with the corresponding eigenvector $\bar{1}$ containing all ones. In other words, the Laplacian matrix $\bar{\bar{\mathbf{L}}}$ has a one-dimensional null-space spanned by vector $\bar{1}$. We can denote eigenvalues of the Graph G by $\sigma_1(G)$, $\sigma_2(G)$, …, $\sigma_N(G)$ with the following assumption:

$$\sigma_1(G) \geq \sigma_2(G) \geq \ldots \geq \sigma_N(G) = 0. \tag{5}$$

As for a connected graph without isolated vertices or components, $\sigma_{N-1}(G)$ is the smallest nonzero eigenvalue [15,16]. Here, we call the (N-1) × (N-1) submatrix, obtained by deleting row i and column i of the Laplacian matrix, principal submatrix. It is easy to prove that the principal submatrix is of full rank when the graph is connected.

The number of loop basis functions has been explicitly investigated in [5]. It is obvious that the matrix $\bar{\bar{\mathbf{\Lambda}}}^T \bar{\bar{\mathbf{\Lambda}}}$ is the principal submatrix of the Laplacian matrix associated with the graph constituted by nodes and edges

of the mesh in the closed structure.

The RWG-connected graph can also be analyzed in a similar manner. By deleting edges between two nodes and drawing lines between RWG-connected vertices, a companion graph can be obtained. As shown in Fig. 2 (b), where three subgraphs are drawn with solid lines using different colors in the RWG-connected graph which is the companion one of the edge-connected graph in Fig. 2 (a). In the companion graph, there are at most three isolated subgraphs [11], while vertices are connected in every subgraph. Assume that the number of the subgraph is N_s and the flower to RWG base transformation matrices in every subgraphs are denoted by $\overline{\overline{\mathbf{F}}}_i$, then it follows:

$$\overline{\overline{\mathbf{F}}}_i^T \overline{\overline{\mathbf{F}}}_j = \overline{\overline{\mathbf{0}}} \quad (i, j = 1, ..., N_s;\ i \neq j)\,. \tag{6}$$

The matrix $\overline{\overline{\mathbf{F}}}_i^T \overline{\overline{\mathbf{F}}}_i$ is the principal submatrix of the Laplacian matrix $\overline{\overline{\mathbf{L}}}_i$ corresponding to the i-th subgraph. Given that every subgraph is connected, the smallest eigenvalue of the Laplacian matrix is zero, while the second smallest eigenvalue is positive. In result, the multiplicity of zero eigenvalues of the Laplacian matrix associated with the total RWG-connected graph equals to the number of the subgraph. In order to make sure that flower basis functions are linearly independent, one node should be dropped in every subgraph, consequently, N_s nodes must be dropped in total.

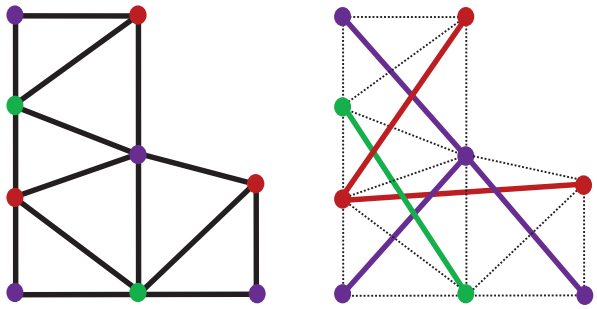

(a) (b)

Fig. 2. Graphs generated using the same mesh nodes: (a) edge-connected graph, and (b) RWG-connected graph.

III. ELECTRIC FIELD INTEGRAL EQUATION WITH LOOP-FLOWER BASIS FUNCTIONS

Consider the problem of electromagnetic wave scattering by three dimensional perfectly conducting surface Ω. The scatter fields ($\boldsymbol{E}^s$, $\boldsymbol{H}^s$) are generated by surface current $\boldsymbol{J}(\boldsymbol{r})$. The EFIE can be written by:

$$\mathcal{T}(\boldsymbol{J}) = -\hat{\boldsymbol{n}} \times \boldsymbol{E}^{inc}\,, \tag{7}$$

where $\boldsymbol{E}^{inc}$ is the incident electric field and the EFIE operator $\mathcal{T}$ is defined by:

$$\mathcal{T}(\boldsymbol{J}) = -j\omega\mu\hat{\boldsymbol{n}} \times \int_\Omega \boldsymbol{J}(\boldsymbol{r}')g(\boldsymbol{r}, \boldsymbol{r}')\,\mathrm{d}\Omega + \frac{1}{j\omega\varepsilon}\hat{\boldsymbol{n}} \times \int_\Omega \nabla' \cdot \boldsymbol{J}(\boldsymbol{r}')\nabla g(\boldsymbol{r}, \boldsymbol{r}')\,\mathrm{d}\Omega\,, \tag{8}$$

in which, ω is the angular frequency, μ and ε denote the permeability and the permittivity respectively. By expanding the surface current $\boldsymbol{J}$ using RWG basis functions and applying Galerkin's method to the EFIE, we can obtain the following linear system:

$$\overline{\overline{\mathbf{Z}}} \bullet \overline{\mathbf{I}} = \overline{\mathbf{V}}\,. \tag{9}$$

When the loop-flower decomposition is performed, the surface current satisfies:

$$\boldsymbol{J} = \boldsymbol{J}^L + \boldsymbol{J}^F\,, \tag{10}$$

in which, the two currents satisfy that $\nabla \cdot \boldsymbol{J}^L = 0$, $\nabla \times \boldsymbol{J}^L \neq 0$, $\nabla \cdot \boldsymbol{J}^F \neq 0$ and $\nabla \times \boldsymbol{J}^L \approx 0$, consequently the EFIE (9) can be rewritten by:

$$\begin{bmatrix} \overline{\overline{\mathbf{Z}}}^{LL} & \overline{\overline{\mathbf{Z}}}^{LF} \\ \overline{\overline{\mathbf{Z}}}^{FL} & \overline{\overline{\mathbf{Z}}}^{FF} \end{bmatrix} \begin{bmatrix} \overline{\mathbf{I}}^L \\ \overline{\mathbf{I}}^F \end{bmatrix} = \begin{bmatrix} \overline{\mathbf{V}}^L \\ \overline{\mathbf{V}}^F \end{bmatrix}. \tag{11}$$

In order to obtain stable system, a frequency scaling is adopted as follows:

$$\begin{bmatrix} k^{-1}\overline{\overline{\mathbf{Z}}}^{LL} & \overline{\overline{\mathbf{Z}}}^{LF} \\ \overline{\overline{\mathbf{Z}}}^{FL} & k\overline{\overline{\mathbf{Z}}}^{FF} \end{bmatrix} \begin{bmatrix} \overline{\mathbf{I}}^L \\ k^{-1}\overline{\mathbf{I}}^F \end{bmatrix} = \begin{bmatrix} k^{-1}\overline{\mathbf{V}}^L \\ \overline{\mathbf{V}}^F \end{bmatrix}. \tag{12}$$

After the treatment, the low-frequency breakdown can be overcome, and the conditioning of the impendence matrix can be improved significantly, hence the linear equation system is now solvable even at very low frequencies. From another point of view, loop-flower basis functions can be easily integrated into existing EFIE-MoM codes as if they construct an algebraic preconditioner. Consequently, (9) can be rewritten by:

$$\overline{\overline{\mathbf{P}}}_{PR}\left(\overline{\overline{\mathbf{H}}}_{LF}^T \overline{\overline{\mathbf{Z}}}^{RWG} \overline{\overline{\mathbf{H}}}_{LF}\right) \overline{\overline{\mathbf{P}}}_{PO}\left(\overline{\overline{\mathbf{P}}}_{PO}^{-1} \overline{\mathbf{I}}^{LF}\right) = \overline{\overline{\mathbf{P}}}_{PR} \overline{\overline{\mathbf{H}}}_{LF}^T \overline{\mathbf{V}}^{RWG}\,, \tag{13}$$

where

$$\overline{\overline{\mathbf{P}}}_{PR} = \begin{bmatrix} k^{-1}\overline{\overline{\mathbf{U}}} & \overline{\overline{\mathbf{0}}} \\ \overline{\overline{\mathbf{0}}} & \overline{\overline{\mathbf{U}}} \end{bmatrix}, \tag{14}$$

and

$$\overline{\overline{\mathbf{P}}}_{PO} = \begin{bmatrix} \overline{\overline{\mathbf{U}}} & \overline{\overline{\mathbf{0}}} \\ \overline{\overline{\mathbf{0}}} & k\overline{\overline{\mathbf{U}}} \end{bmatrix}, \tag{15}$$

in which, $\overline{\overline{\mathbf{U}}}$ is the identity matrix, and $\overline{\overline{\mathbf{H}}}^{LF} = [\overline{\overline{\mathbf{\Lambda}}}, \overline{\overline{\mathbf{F}}}]$ denotes loop-flower to RWG basis functions transformation matrix. Finally, the coefficients of RWG basis functions can be obtained by:

$$\overline{\mathbf{I}}^{RWG} = \overline{\overline{\mathbf{H}}}^{LF} \overline{\mathbf{I}}^{LF}\,. \tag{16}$$

IV. LOOP-FLOWER GRAM MATRIX

It can be found in [17] that the Gram matrix of RWG basis functions:

$$(\bar{\bar{\mathbf{G}}})_{i,j} = < \boldsymbol{f}_i, \boldsymbol{f}_j >, \tag{17}$$

is well-conditioned. Here, the inner product is defined by $< \boldsymbol{a}, \boldsymbol{b} >= \int_{\Gamma} \boldsymbol{a} \bullet \boldsymbol{b} \, \mathrm{d}\Gamma$. The Gram matrix of RWG basis functions has the same conditioning property as the identity matrix [12,17].

Since loop and star coefficient matrices are orthogonal [5], in addition, flower basis functions are actually the linear combinations of star basis functions surrounding their reference nodes, it can be validated that loop and flower coefficient matrices are also orthogonal between each other. Loop and flower Gram matrices can be written by:

$$\{\bar{\bar{\mathbf{G}}}^L\}_{i,j} = \{\bar{\bar{\mathbf{\Lambda}}}^T \bar{\bar{\mathbf{G}}} \bar{\bar{\mathbf{\Lambda}}}\}_{i,j} = < \boldsymbol{f}_i^L, \boldsymbol{f}_j^L >, \tag{18}$$

$$\{\bar{\bar{\mathbf{G}}}^F\}_{i,j} = \{\bar{\bar{\mathbf{F}}}^T \bar{\bar{\mathbf{G}}} \bar{\bar{\mathbf{F}}}\}_{i,j} = < \boldsymbol{f}_i^F, \boldsymbol{f}_j^F >, \tag{19}$$

respectively, here $\{\bar{\bar{\mathbf{G}}}^L\}_{i,j}$ means the (i, j) element of matrix $\bar{\bar{\mathbf{G}}}^L$. According to above discussion, the Gram matrix of loop-flower basis functions has the following relationship:

$$\begin{aligned} \bar{\bar{\mathbf{G}}}^{LF} &= \bar{\bar{\mathbf{H}}}_{LF}^T \bar{\bar{\mathbf{G}}} \bar{\bar{\mathbf{H}}}_{LF} \asymp \bar{\bar{\mathbf{H}}}_{LF}^T \bar{\bar{\mathbf{H}}}_{LF} = \begin{pmatrix} \bar{\bar{\mathbf{\Lambda}}}^T \bar{\bar{\mathbf{\Lambda}}} & \bar{\bar{\mathbf{0}}} \\ \bar{\bar{\mathbf{0}}} & \bar{\bar{\mathbf{F}}}^T \bar{\bar{\mathbf{F}}} \end{pmatrix} \\ &\asymp \begin{pmatrix} \bar{\bar{\mathbf{\Lambda}}}^T \bar{\bar{\mathbf{G}}} \bar{\bar{\mathbf{\Lambda}}} & \bar{\bar{\mathbf{0}}} \\ \bar{\bar{\mathbf{0}}} & \bar{\bar{\mathbf{F}}}^T \bar{\bar{\mathbf{G}}} \bar{\bar{\mathbf{F}}} \end{pmatrix} = \begin{pmatrix} \bar{\bar{\mathbf{G}}}^L & \bar{\bar{\mathbf{0}}} \\ \bar{\bar{\mathbf{0}}} & \bar{\bar{\mathbf{G}}}^F \end{pmatrix} \end{aligned}. \tag{20}$$

The notation $\bar{\bar{\mathbf{A}}} \asymp \bar{\bar{\mathbf{B}}}$ denotes that there exist two constant numbers C_1 and C_2 such that $C_1 \bar{\mathbf{v}}^T \bar{\bar{\mathbf{B}}} \bar{\mathbf{v}} \le \bar{\mathbf{v}}^T \bar{\bar{\mathbf{A}}} \bar{\mathbf{v}} \le C_2 \bar{\mathbf{v}}^T \bar{\bar{\mathbf{B}}} \bar{\mathbf{v}}$ holds true for every arbitrary vector $\bar{\mathbf{v}}$, which means that spectral properties between matrix $\bar{\bar{\mathbf{A}}}$ and $\bar{\bar{\mathbf{B}}}$ are equivalent. After investigating (20), we can find that the Gram matrix of loop-flower basis functions has the equivalent conditioning behavior of the block diagonal matrix with two block elements which are Gram matrices of loop basis functions and flower basis functions. So we can analyze the two block elements separately to obtain the total conditioning property of the Gram matrix of loop-flower basis functions. Assume that the surface of a concerned object is discretized using uniform triangular mesh with average edge length *h*, it has been presented in [17] that:

$$\mathrm{cond}(\bar{\bar{\mathbf{G}}}^L) \asymp \frac{1}{h^2}, \tag{21}$$

holds true for both closed and open objects. In addition, $\mathrm{cond}(\bar{\bar{\mathbf{G}}}^L)$ should be interpreted as the reduced condition number $\sigma_1(\bar{\bar{\mathbf{G}}}^L)/\sigma_{Nl-1}(\bar{\bar{\mathbf{G}}}^L)$ when the closed structure is analyzed and meshed with *Nl* loop basis functions. Since the number of the triangular mesh is subject to $N_h \asymp 1/h^2$, we can also find that $\mathrm{cond}(\bar{\bar{\mathbf{G}}}^L) \asymp N_h$. For more details associated with the conditioning of loop Gram matrix, the reader should refer to [17,18] and references therein.

From (18), (20) and (21), it follows that:

$$\mathrm{cond}(\bar{\bar{\mathbf{\Lambda}}}^T \bar{\bar{\mathbf{\Lambda}}}) \asymp \frac{1}{h^2}, \tag{22}$$

where $\bar{\bar{\mathbf{\Lambda}}}^T \bar{\bar{\mathbf{\Lambda}}}$ is the principal submatrix of the Laplacian matrix. We can also obtain that:

$$\sigma_1(\bar{\bar{\mathbf{\Lambda}}}^T \bar{\bar{\mathbf{\Lambda}}}) \asymp 1 \text{ and } \sigma_{Nl-1}(\bar{\bar{\mathbf{\Lambda}}}^T \bar{\bar{\mathbf{\Lambda}}}) \asymp h^2. \tag{23}$$

The analysis of $\bar{\bar{\mathbf{G}}}^F$ can be traced to the analysis of $\bar{\bar{\mathbf{G}}}^L$. Given that the RWG Gram matrix is well-conditioned, the matrix $\bar{\bar{\mathbf{G}}}^F$ maintains the following equivalences:

$$\bar{\bar{\mathbf{G}}}^F = \bar{\bar{\mathbf{F}}}^T \bar{\bar{\mathbf{G}}} \bar{\bar{\mathbf{F}}} \asymp \bar{\bar{\mathbf{F}}}^T \bar{\bar{\mathbf{F}}}, \tag{24}$$

so that we can analyze the principal submatrix $\bar{\bar{\mathbf{F}}}^T \bar{\bar{\mathbf{F}}}$ of the Laplacian matrix $\bar{\bar{\mathbf{L}}}$ of the RWG-connected graph instead. For the sake of brevity, here we assume that there are three RWG-connected subgraphs in the mesh structure. According to the discussion in the previous section, the flower coefficient matrix $\bar{\bar{\mathbf{F}}}$ can be expressed by:

$$\bar{\bar{\mathbf{F}}} = [\bar{\bar{\mathbf{F}}}_1, \bar{\bar{\mathbf{F}}}_2, \bar{\bar{\mathbf{F}}}_3], \tag{25}$$

and the principal submatrix $\bar{\bar{\mathbf{F}}}^T \bar{\bar{\mathbf{F}}}$ turns to be:

$$\bar{\bar{\mathbf{F}}}^T \bar{\bar{\mathbf{F}}} = \begin{pmatrix} \bar{\bar{\mathbf{F}}}_1^T \bar{\bar{\mathbf{F}}}_1 & \bar{\bar{\mathbf{0}}} & \bar{\bar{\mathbf{0}}} \\ \bar{\bar{\mathbf{0}}} & \bar{\bar{\mathbf{F}}}_2^T \bar{\bar{\mathbf{F}}}_2 & \bar{\bar{\mathbf{0}}} \\ \bar{\bar{\mathbf{0}}} & \bar{\bar{\mathbf{0}}} & \bar{\bar{\mathbf{F}}}_3^T \bar{\bar{\mathbf{F}}}_3 \end{pmatrix}, \tag{26}$$

where $\bar{\bar{\mathbf{F}}}_i^T \bar{\bar{\mathbf{F}}}_i$ is the principal submatrix of the Laplacian matrix $\bar{\bar{\mathbf{L}}}_i$ corresponding to the subgraph G_i that is connected. According to Cauchy interlacing theorem in [16,19], we can get the following spectral inequality:

$$\begin{aligned} &\sigma_1(\bar{\bar{\mathbf{L}}}_i) \ge \sigma_1(\bar{\bar{\mathbf{F}}}_i^T \bar{\bar{\mathbf{F}}}_i) \ge \sigma_2(\bar{\bar{\mathbf{L}}}_i) \ge \sigma_2(\bar{\bar{\mathbf{F}}}_i^T \bar{\bar{\mathbf{F}}}_i) \ge \ldots \\ &\ge \sigma_{N_1-1}(\bar{\bar{\mathbf{L}}}_i) \ge \sigma_{N_1-1}(\bar{\bar{\mathbf{F}}}_i^T \bar{\bar{\mathbf{F}}}_i) \ge \sigma_{N_1}(\bar{\bar{\mathbf{L}}}_i) = 0 \end{aligned}. \tag{27}$$

Since the maximum singular value of the Laplacian matrix $\bar{\bar{\mathbf{L}}}_i$ is bounded by:

$$\begin{aligned} &d(u) + 1 \le \sigma_1(\bar{\bar{\mathbf{L}}}_i) \\ &\le \max\{d(u) + d(v) \mid (u, v) \in E(G_i)\} \end{aligned}, \tag{28}$$

where *u* and *v* are two vertices of arbitrary edges in the graph G_i, and $d(u)$ means the degree associated with the vertex *u* [15], so that the maximum singular value of $\bar{\bar{\mathbf{F}}}_i^T \bar{\bar{\mathbf{F}}}_i$ is also bounded. From the inequality (27), it is

obvious that the smallest eigenvalue is rather small and becomes an isolated singular value from the perspective of quantity. The isolated singular value is irrelevant for iterative solution [17], so that we can use the reduced condition number, which is the ratio between the maximum singular value and second smallest one, to estimate the global convergence.

Consider that RWG-connected relation behaves similarly to edge-connected relation in the analysis of loop basis functions, we can also obtain that:

$$\sigma_1(\bar{\bar{\mathbf{F}}}_i^T\bar{\bar{\mathbf{F}}}_i) \asymp 1 \text{ and } \sigma_{Nfi-1}(\bar{\bar{\mathbf{F}}}_i^T\bar{\bar{\mathbf{F}}}_i) \asymp h^2, \tag{29}$$

so that,

$$\text{cond}(\bar{\bar{\mathbf{F}}}^T\bar{\bar{\mathbf{F}}}) \asymp \frac{1}{h^2}. \tag{30}$$

From (24) and (30), it follows that:

$$\text{cond}(\bar{\bar{\mathbf{G}}}^F) \asymp \frac{1}{h^2}. \tag{31}$$

In result, from (20), (21) and (31),

$$\text{cond}(\bar{\bar{\mathbf{G}}}^{LF}) \asymp \frac{1}{h^2}. \tag{32}$$

In fact, the transformation matrix $\bar{\bar{\mathbf{F}}}$ is defined on the total nodes in the mesh except no more than three discarded nodes and the number of the discarded nodes equals to the multiplicity of zero eigenvalue of the Laplacian matrix associated with the RWG-connected graph. Furthermore, the discarded nodes can be selected and dropped according to the algorithm in [11].

V. NUMERICAL RESULTS

This section presents numerical tests that corroborate the theory developed in the previous sections. The efficiency and accuracy of loop-flower basis functions have been validated by a scattering example. Unless otherwise specified, the simulations are run on a personal computer equipped with four Core Intel(R) Core(TM) i5-4440 CPU at 3.10 GHz and 8 GB of RAM.

A. Conditioning of loop-flower Gram matrices

The first test illustrates the validity of spectral properties of the principal submatrix corresponding to the Laplacian matrix associated with the RWG-connected graph. The test is conducted with a 1m×1m PEC square plate discretized by using different uniform meshes. It is obvious in Fig. 3 that the maximum singular value is bounded and the upper bound is about 10, while the second smallest singular value decays in the same order of h^2. In addition, the smallest value is vanishingly small.

Figure 4 shows the reduced condition numbers for loop-flower Gram matrices in both closed and open structures. In Fig. 4 (a), the reduced condition number of the loop-flower Gram matrix corresponding to the above square plate is presented. The results indicates that the reduced condition number of the loop-flower Gram matrix has a predicted growth of h^{-2}. Additionally, the loop-flower Gram matrix associated with a PEC sphere discretized with several uniform meshes is also investigated. Figure 4 (b) shows that the reduced condition number of the loop-flower Gram matrix associated with a sphere also grows theoretically as h^{-2}.

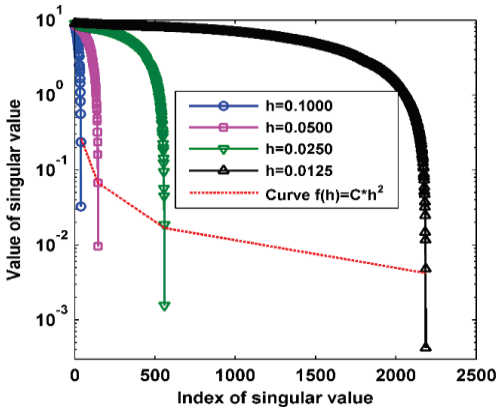

Fig. 3. Singular value of principal submatrix.

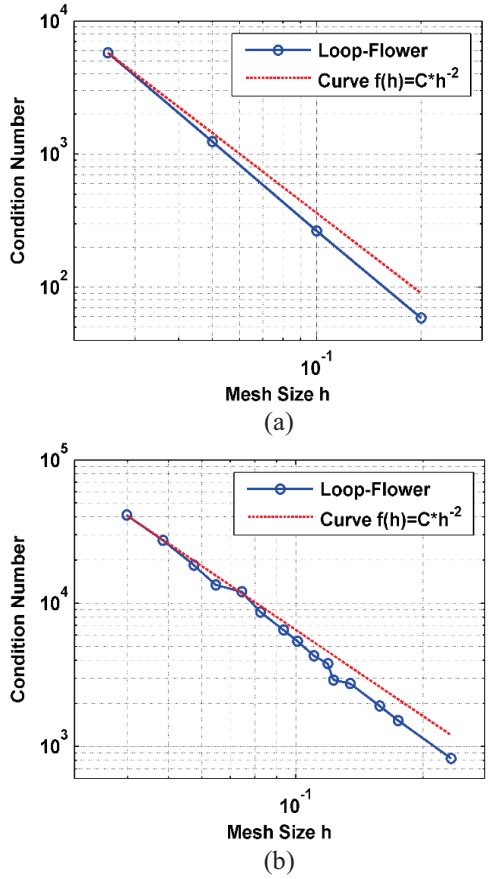

Fig. 4. Reduced condition number of loop-flower Gram matrix: (a) square plate, and (b) sphere.

B. Performance of loop flower basis functions

In this part, the structures are under the excitation of x-polarized plane waves with amplitude of 1 V/m and frequency of 300 Hz, traveling along $-z$ axis.

A PEC cylinder is analyzed in this part. The radius of the cylinder is 0.5 m and the height is 2 m. The surface mesh contains 3372 triangles, 5058 edges and 1688 nodes. Figure 5 shows the RCS calculated by LS bases, LF bases. The result obtained by LF bases agrees well with LS bases.

Convergence results for LS bases and LF basis functions are given in Fig. 6 with conjugate gradient (CG) iteration. It can be seen that iteration associated with LF bases converge fast compared with LS basis functions. It took the LS bases 154920 times of iterations to achieve a relative residual error of 10^{-6}, while LF bases 4203 times of iterations.

Furthermore, the total CPU time of LS solver is 13350 seconds, which is about 30 times more than LF with the CPU time of 453 seconds only.

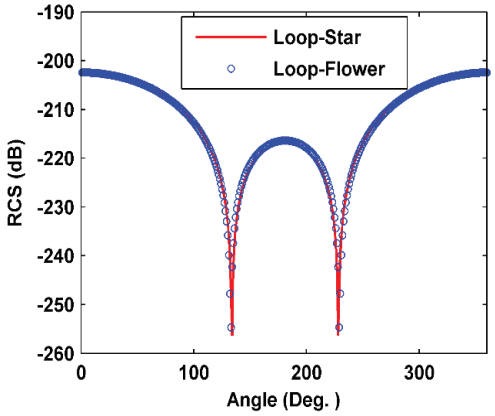

Fig. 5. BiRCS solutions for a PEC cylinder when the frequency equals to 300 Hz.

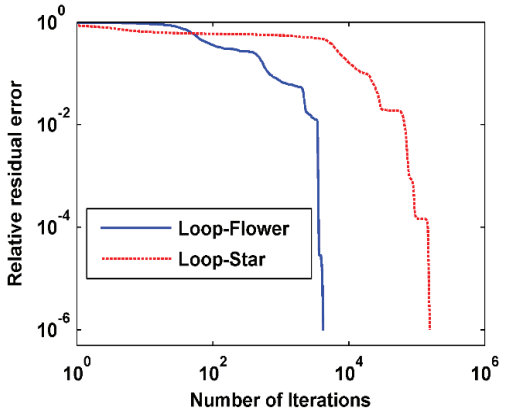

Fig. 6. Relative residual error versus number of iterations for a PEC cylinder scattering problems when frequency is 300 Hz.

VI. CONCLUSION

We have analyzed flower basis functions based on RWG-connected graphs which are generated according to RWG basis functions. The number of zero eigenvalues of the Laplacian matrix associated with the RWG-connected graph equals to the number of redundant nodes of flower basis functions. In addition, the maximum singular value of flower Gram matrix is bounded, and the reduced condition number of flower Gram matrix grows as h^{-2}. Furthermore, the reduced condition number of loop-flower basis functions also has a growth as h^{-2} and the condition behavior of the Gram matrix becomes worse with increase of the mesh density.

Loop-flower basis functions are efficient to overcome the low frequency breakdown. Compared with loop-star basis functions, the linear EFIE system with loop-flower basis functions has a better conditioning. The numerical results demonstrate the excellent performance of loop-flower basis functions.

ACKNOWLEDGMENT

This work is supported by the SAST foundation 2013.

REFERENCES

[1] F. P. Andriulli, A. Tabacco, and G. Vecchi, "Solving the EFIE at low frequencies with a conditioning that grows only logarithmically with the number of unknowns," *IEEE Trans. Antennas Propagat.*, vol. 58, no. 5, pp. 1614-1624, May 2010.

[2] S. B. Adrian, F. P. Andriulli, and T. F. Eibert, "Hierarchical bases preconditioners for the electric filed integral equation on multiply connected geometries," *IEEE Trans. Antennas Propagat.*, vol. 62, no. 11, pp. 5856-5861, Nov. 2014.

[3] F. P. Andriulli, K. Cools, I. Bogaert, and E. Michielssen, "On a well-conditioned electric field integral operator for multiply connected geometries," *IEEE Trans. Antennas Propagat.*, vol. 61, no. 4, pp. 2077-2087, Apr. 2013.

[4] M. Burton and S. Kashyap, "A study of a recent, moment-method algorithm that is accurate to very low frequencies," *Appl. Computat. Electromagn. Soc. J.*, vol. 10, no. 3, pp. 58-68, Nov. 1995.

[5] G. Vecchi, "Loop-star decomposition of basis functions in the discretization of the EFIE," *IEEE Trans. Antennas Propagat.*, vol. 47, no. 2, pp. 339-346, Feb. 1999.

[6] J.-F. Lee and R. J. Burkholder, "Loop star basis functions and a robust preconditioner for EFIE scattering problems," *IEEE Trans. Antennas Propagat.*, vol. 51, no. 8, pp. 1855-1863, Aug. 2003.

[7] J.-S. Zhao and W. C. Chew, "Integral equation solution of Maxwell's equations from zero

frequency to microwave frequencies," *IEEE Trans. Antennas Propagat*., vol. 48, no. 10, pp. 1635-1645, Oct. 2000.

[8] T. F. Eibert, "Iterative-solver convergence for loop-star and loop-tree decompositions in method-of-moments solutions of the electric-field integral equation," *IEEE Antennas Propagation Magazine*, vol. 46, no. 3, pp. 80-85, Jun. 2004.

[9] F. P. Andriulli, K. Cools, H. Bagci, F. Olyslager, A. Buffa, S. Christiansen, and E. Michielssen, "A multiplicative Calderon preconditioner for the electric field integral equation,". *IEEE Trans. Antennas Propagat*., vol. 56, no. 8, pp. 2398-2412, Aug. 2008.

[10] A. Buffa and S. H. Christiansen, "A dual finite element complex on the barycentric refinement," *Mathematics of Computation*, vol. 76, no. 260, pp. 1743-1769, Oct. 2007.

[11] G. Xiao, "Applying loop-flower basis functions to analyze electromagnetic scattering problems of PEC scatterers," *Int. J. Antennas Propag*., vol. 2014, pp. 9, article ID 905925, 2014.

[12] Y. Hou and G. Xiao, "Properties of the Gram matrices associated with loop-flower basis functions," *PIERS Proceedings*, Guangzhou, China, pp. 2316-2321, Aug. 2014.

[13] X. Tian, G. Xiao, and J. Fang, "Application of loop-flower basis functions in the time-domain electric field integral equation," *IEEE Trans. Antennas Propagat*., vol. 63, no. 3, pp. 1178-1181, Mar. 2015.

[14] A. Brualdi Richard, *The Mutually Beneficial Relationship of Graphs and Matrices*, vol. 115, American Mathematical Soc., 2011.

[15] R. Grone, R. Merris, and V. S. Sunder, "The Laplacian spectrum of a graph," *SIAM Journal on Matrix Analysis and Applications*, vol. 11, no. 2, pp. 218-238, 1990.

[16] X. D. Zhang, "The Laplacian eigenvalues of graphs: a survey," *arXiv preprint arXiv: 1111.2897*, 2011.

[17] F. P. Andriulli, "Loop-star and loop-tree decompositions: analysis and efficient algorithms," *IEEE Trans. Antennas Propagat*., vol. 60, no. 5, pp. 2347-2356, May 2012.

[18] A. Quarteroni and A. Valli, *Numerical Approximation of Partial Differential Equations*, Berlin: Springer, 1997.

[19] D. Carlson, "Minimax and interlacing theorems for matrices," *Linear Algebra and its Applications*, vol. 54, pp. 153-172, 1983.

Yibei Hou received the B.S. degree from University of Electronic Science and Technology of China (UESTC), Chengdu, China, in 2014, and is currently pursuing the Ph.D. degree in Electronic Engineering at Shanghai Jiao Tong University, Shanghai, China. His research interests include computational electromagnetics and its application in scattering and radiation problems.

Gaobiao Xiao received the M.S. degree from Huazhong University of Science and Technology, Wuhan, China, in 1988, the B.S. degree from the National University of Defense Technology, Changsha, China, in 1991, and the Ph.D. degree from Chiba University, Chiba, Japan, in 2002. He worked in Hunan University, Changsha, China, from 1991 to 1997. Since April 2004, he has been a Faculty Member in the Department of Electronic Engineering, Shanghai Jiao Tong University, Shanghai, China. His research interests are numerical methods in electromagnetic fields, coupled thermo-electromagnetic analysis, microwave filter designs, fiber-optic filter designs, and inverse scattering problems.

Jinpeng Fang received his M.E. from Shanghai Jiao Tong University, Shanghai, China, in 2010. From 2010 on, he's worked as a RF Engineer of Shanghai Key Laboratory of Electromagnetic Environmental Effects for Aerospace Vehicle. His main research interests include simulation and measurement of the effect of electromagnetic environment, electromagnetic scattering properties of objects.